JOURNAL OF MAGNETIC RESONANCE **125,** 102–106 (1997)
ARTICLE NO. MN961076

# Accurate Numerical Approximation to the Gauss–Lorentz Lineshape

J.-P. GRIVET

*Centre de Biophysique Moléculaire, CNRS, Université d'Orléans, rue Charles-Sadron, 45071 Orléans cedex 2, France*

Received August 21, 1996; revised November 12, 1996

**The Gauss–Lorentz lineshape often observed in EPR or NMR is shown to be simply related to the complex error function. Using numerical algorithms developed for the evaluation of this function, experimental lineshapes can be accurately and rapidly simulated. Formulas are presented for the derivatives of the line profile with respect to the parameters and for the approximate computation of the overall linewidth. It is observed that accurate integrals require use of a wide integration interval.** 

## INTRODUCTION

The Gauss–Lorentz lineshape is defined mathematically as the convolution product of Gaussian and Lorentzian functions. It has a long history in magnetic resonance. Portis (*1*) showed that inhomogeneously broadened ESR lines had a Gauss–Lorentz profile. Many workers have presented methods for deconvoluting ESR lines and recovering the physically significant Lorentzian (spin-packet) width. For instance, a computational procedure was described by Ramani *et al.* (*2*) and by Korb and Maruani (*3*). In the case of Fourier transform NMR, the use of a window function consisting of the product of an increasing exponential times a decreasing Gaussian has been advocated by Ernst (*4*) and by Ferridge and Lindon (*5*). After Fourier transformation, the spectrum displays Gauss–Lorentz lineshapes. A graph of the resulting empirical linewidth has recently been presented by Ogg *et al.* (*6*).

The Gauss–Lorentz lineshape has an even older history in gas-phase atomic spectroscopy, where it is known as the Voigt profile (*7*). It arises because the natural atomic lineshape (a Lorentzian) is convoluted with a Gaussian due to Doppler broadening. Simulations of stellar atmospheres require very accurate and fast computations of absorption coefficients. In response to that need, many properties of the Voigt function have been studied and many algorithms have been developed for its evaluation (*8*). It is the purpose of this report to draw the attention of magnetic resonance specialists to this vast body of knowledge and to point to some useful applications.

The classical Voigt function is the Fourier transform of the product of a decreasing exponential by a Gaussian. In high-resolution NMR, increasing exponential factors are also encountered when the window function overcompensates for the signal decay. This produces negative lobes on either side of the line. These artifacts are often tolerated, because the central part of the signal is quite narrow and well resolved. This lineshape can also be easily computed by using a generalization of the Voigt function known as the plasma dispersion function (*9*) or the complex error function (*10*). This function provides the added benefit that the imaginary part of the spectrum can be computed with little additional effort. Ill-phased lines can then be simulated by suitably combining real and imaginary parts.

We will first make the connection between the NMR Gauss–Lorentz lineshape and the complex error function. We will then compare some experimental and computed line profiles. We will show how the Voigt linewidth can be easily estimated. We end with a caveat on the integrals of Gauss–Lorentz lines.

## MATHEMATICAL DEVELOPMENT

We consider an NMR signal, (FID) $s(t)$, which can be assumed without loss of generality to have zero frequency and unit initial amplitude,

$$\begin{aligned} s(t) &= 0, && t < 0, \\ &= \exp(-t/T_2^*), && t \geqslant 0, \end{aligned} \qquad [1]$$

where $T_2^*$ is the effective decay time of the FID. Its Fourier transform is the spectrum $S(\nu)$:

$$S(\nu) = \frac{1}{T_2^*}\,\frac{1}{4\pi^2\nu^2 + (1/T_2^*)^2} - \frac{2i\pi\nu}{4\pi^2\nu^2 + (1/T_2^*)^2}.$$

The real part is a Lorentzian having full width $1/\pi T_2^*$ at



1090-7807/97 $25.00

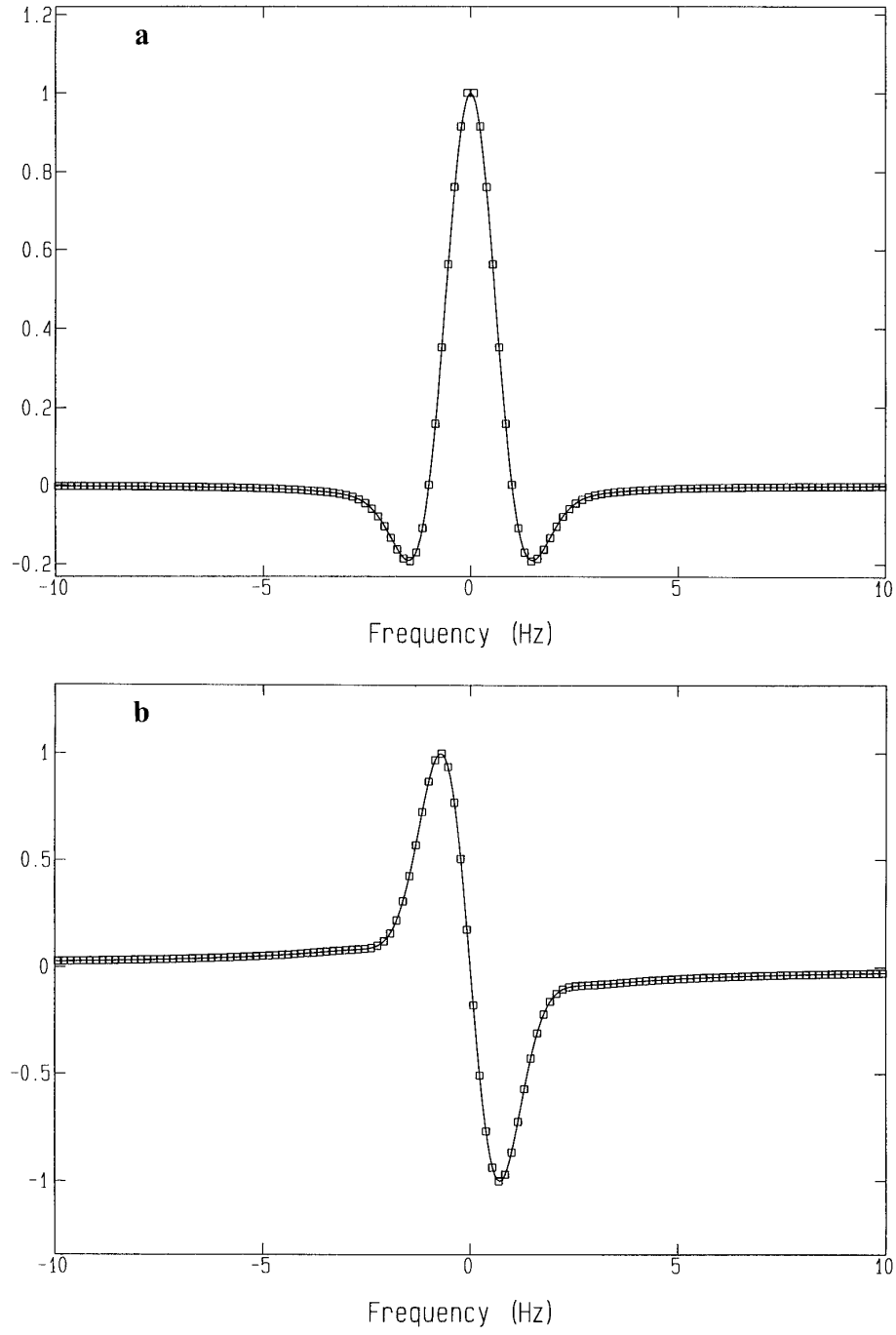


**FIG. 1.** FFT of a synthetic FID (full line) and values [open squares, computed according to Ref. (*11*)] for a Gauss–Lorentz line: (a) real part; (b) imaginary part. The natural width was taken as 2 Hz. The FID was multiplied by an increasing exponential (equivalent width −4 Hz) and a Gaussian (width 2 Hz); 1024 complex points were used in the FFT, for a spectral width of 123 Hz.

half-maximum. It is interesting to note that the Fourier transform of a Gaussian signal

$$\begin{aligned} s(t) &= 0, & t < 0, \\ &= \exp(-at^2), & t \geqslant 0 \end{aligned}$$

cannot be expressed in terms of elementary functions; it is given by

$$S(\nu) = \sqrt{\frac{\pi}{a}}\, e^{-\pi^2\nu^2/a} + \frac{i}{\sqrt{a}}\, e^{-\pi^2\nu^2/a} \int_0^{\pi\nu/\sqrt{a}} e^{s^2} ds.$$

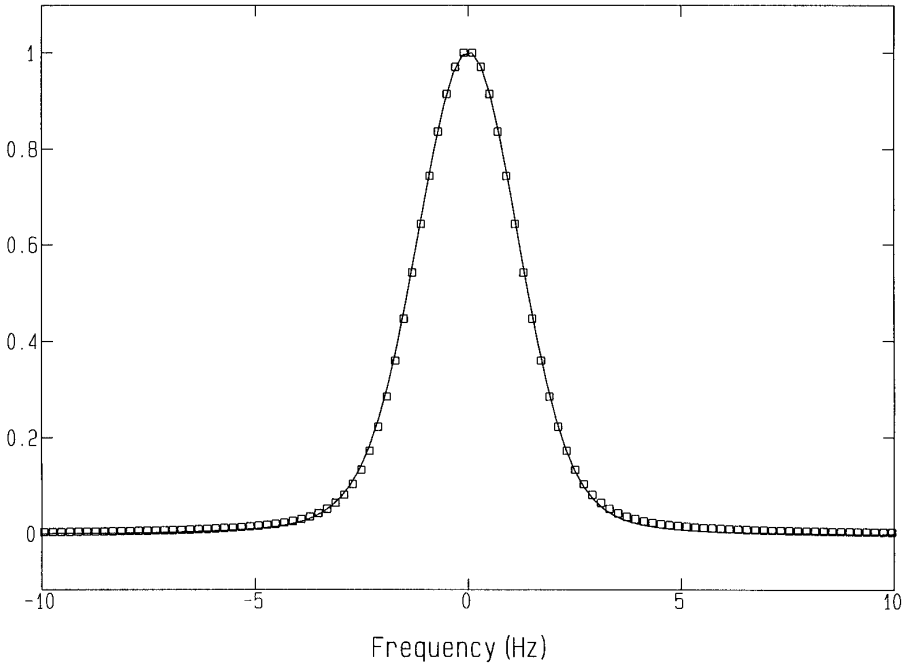


**FIG. 2.** Experimental (full line) and computed (open squares) normalized lineshape of $^1H^2HO$ in $^2H_2O$. The natural linewidth was 0.7 Hz, and the FID was multiplied by an increasing exponential (equivalent width −0.03 Hz) and a Gaussian (width 2.4 Hz) before Fourier transformation and manual phasing. The digital resolution was 0.22 Hz. The same filter parameters were used in the simulation.

The real part is a Gaussian with full width at half-maximum of $\lambda_G = (2/\pi)\sqrt{a \ln 2}$. The imaginary part is known as Dawson's integral (*10*, Chap. 7). Let us now consider the mixed Lorentz–Gauss case, which may be formulated as follows. Before Fourier transformation, the FID, given by Eq. [1], is multiplied by an exponential $\exp(-t/T_f)$, with $\lambda_f = 1/\pi T_f$, and by a Gaussian, $\exp(-at^2)$. We introduce the parameter $\beta = 1/T_2^* + 1/T_f$; $\beta$ can be of either sign. The spectrum is now given by

$$S(\nu) = \int_0^\infty e^{-at^2-\beta t-2i\pi\nu t}dt.$$

Using formula 7.4.2 of (*10*), with $c = 0$ and $b = \beta/2 + i\pi\nu$, we obtain

$$S(\nu) = \frac{1}{2}\sqrt{\frac{\pi}{a}}\, w\left(\frac{\pi\nu}{\sqrt{a}} + \frac{i\beta}{2\sqrt{a}}\right),$$

where $w(x + iy)$ is the complex error function of a complex argument which is defined as (*10*)

$$w(z) = e^{-z^2}erfc(-iz); \quad erfc(z) = \frac{2}{\sqrt{\pi}}\int_z^\infty e^{-t^2}dt.$$

The numerical computation of $S$ or $w$ is easily achieved with any of the algorithms analyzed by Schreier (*8*). We have used the simple formulation of Hui *et al.* (*11*). These authors report a relative accuracy of better than $10^{-4}$ over the entire $x$, $y$ plane, which is quite sufficient for our purposes. The corresponding PASCAL program is available from the author.

## COMPARISON WITH THE NUMERICAL FOURIER TRANSFORM

We have synthesized FIDs of different decay times, multiplied them by Lorentz–Gauss windows, and, using an FFT program, obtained the corresponding spectra; the same parameters were used in the Hui algorithm. In each case, we obtained perfect agreement between the two methods: an example of such a comparison is shown in Fig. 1. We expect that the two methods give identical results as long as (i) truncation and (ii) digitization effects can be neglected; (i) is not a serious limitation since, in most applications, the Gaussian function falls off rapidly at long times, and (ii) can be minimized by zero filling.

The algorithm of Hui *et al.* comprises ten complex multiplications and one complex division per frequency point; it is thus faster than the FFT if only a single line is to be simulated. Schreier (*8*) provides a detailed but somewhat inconclusive discussion of computation times for the case of a multiline spectrum. We believe that the availability

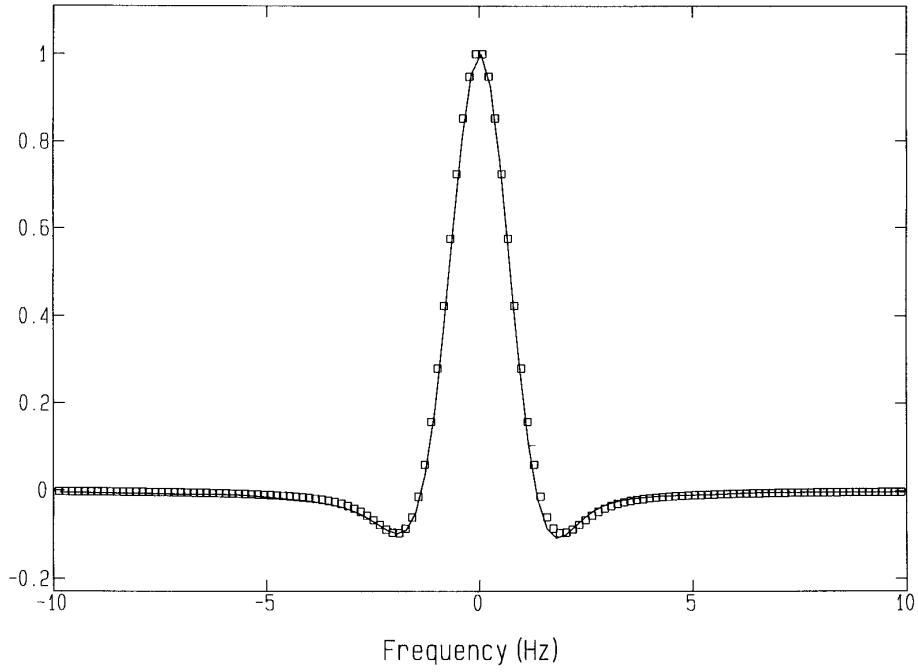


**FIG. 3.** (Full line) The same FID as in Fig. 2 was multiplied by an increasing exponential (equivalent width −1.3 Hz) and a Gaussian (width 2 Hz) and Fourier transformed. (Open squares) Computed lineshape, using the same parameters and the algorithm of Hui *et al.* (*11*).

of derivatives of the lineshape with respect to the window parameters (see below) is an added advantage.

## EXPERIMENTAL VERIFICATION

The resonance line of residual water in $D_2O$ was recorded in a 5 mm tube at 300.13 MHz, using quadrature detection with 4096 data points, for a spectral width of 900 Hz. The FID was zero-filled to 8K points, multiplied by a filter function, Fourier transformed, and manually phased. The natural linewidth of the unwindowed spectrum was found to be 0.7 Hz ($T_2^* = 0.455$ s). The Bruker software defines the Gaussian function in terms of the abscissa on the time axis (defined as a fraction ''GB'' of the acquisition time ''AQ'') where the window is maximum. The constant $a$ is therefore

$$a = 1/(2 \cdot |T_f| \cdot \mathrm{GB} \cdot \mathrm{AQ}).$$

The spectra were transferred to a desktop computer for comparison with computed lineshapes. Two representative absorption spectra and their simulations are shown in Figs. 2 and 3. For both, the acquisition time is 2.273 s. Figure 2 shows the case $\lambda_f = -0.03$ Hz, so that $\beta$ is positive ($\beta = 2.105\ s^{-1}$) while the width due to the Gaussian filter is 2.4 Hz (GB = 0.001, $a = 20.5\ s^{-2}$). Figure 3 displays a spectrum for which $\lambda_f = -2$ Hz; $\beta$ is now negative ($\beta = -4.08\ s^{-1}$). The Gaussian filter broadening is 2 Hz (GB = 0.1, $a = 14.2\ s^{-2}$). It can be seen that the agreement between experimental and computed spectra is satisfactory.

## LINEWIDTHS

Since the purpose of the Lorentz–Gauss transformation is often resolution enhancement, the resultant linewidth is of interest. For a positive $\beta$, one may use the experimental results of Ogg *et al.* (*6*), but the very simple empirical formula of Whiting (*12*) can also be used, with a reported maximum error of 1.5% (*13*). The full width at half-maximum of the Voigt profile is given in terms of the width of the Lorentzian component $\lambda_L = \beta/\pi$ and of the width of the Gaussian $\lambda_G = (2/\pi)\sqrt{a \ln 2}$ by the following relation:

$$\lambda_V = (1/2)[\lambda_L + (\lambda_L^2 + 4\,\lambda_G^2)^{1/2}]. \qquad [2]$$

For example, assuming that $\lambda_L = 2$ Hz and $\lambda_G = 4$ Hz, [2] gives $\lambda_V = 5.1$ Hz, to be compared with a computed value of 5.2 Hz and an experimental value of 5.3 Hz (*6*). For the line of Fig. 2, we measure 2.84 Hz, and formula [2] predicts 2.78 Hz, a discrepancy much smaller than the digital resolution of 0.22 Hz.

## DERIVATIVES AND INTEGRAL OF THE VOIGT FUNCTION

Nonlinear least-squares algorithms are frequently used to retrieve line frequencies and intensities. Their implementa-

tion requires a knowledge of the derivatives of the lineshape with respect to the parameters. As the function $w(z)$ satisfies the simple differential equation

$$w'(z) = \frac{2i}{\sqrt{\pi}} - 2zw(z),$$

the computation of derivatives of $w$ is straightforward (*8*). Setting $w(x,y) = A(x,y) + iD(x,y)$, the following results are obtained:

$$\frac{\partial A}{\partial x} = -2\mathrm{Re}(zw); \qquad \frac{\partial A}{\partial y} = -\frac{2}{\sqrt{\pi}} + 2\ \mathrm{Im}(zw);$$

$$\frac{\partial D}{\partial x} = \frac{2}{\sqrt{\pi}} - 2\ \mathrm{Im}(zw); \quad \frac{\partial D}{\partial y} = -2\ \mathrm{Re}(zw).$$

The integral of $A = \mathrm{Re}(w)$ over the entire real axis is unity, since both the FID and the window function are equal to 1 for $t = 0$. However, when the real parts of the simulated spectra shown in the figures are numerically integrated, results slightly different from 1 are obtained: 0.98 for Fig. 2 and 1.04 for Fig. 3. This is due to the asymptotic behavior of the function $w(z)$ which behaves as $i/z$ for large $z$ (*9*), so that $A(x,y) \sim 1/(x^2 + y^2)$, just as for a pure Lorentzian. Only when $y = 0$ exactly do these extended wings vanish; $A(x,0)$ is then rigorously a Gaussian. The effect is more significant the larger is $y$, so that, for quantitative work, small values of $|y| = |\beta|/2\sqrt{a} = (\ln 2)^{1/2}|\lambda_L|/\lambda_G$ are preferred.

## REFERENCES


1. A. M. Portis, *Phys. Rev.* **91,** 1071 (1953).
2. K. Ramani, S. Ganapathy, and R. Srinivasan, *J. Magn. Reson.* **24,** 231 (1976).
3. J.-P. Korb and J. Maruani, *J. Magn. Reson.* **46,** 514 (1982).
4. R. R. Ernst, *Adv. Magn. Reson.* **2,** 1 (1966).
5. A. G. Ferridge and J. C. Lindon, *J. Magn. Reson.* **31,** 341 (1978).
6. R. J. Ogg, P. B. Kingsley, and J. S. Taylor, *J. Magn. Reson. A* **117,** 113 (1995).
7. A. C. G. Mitchell and M. W. Zamansky, ''Resonance Radiation and Excited Atoms,'' Cambridge Univ. Press, Cambridge, 1934.
8. F. Schreier, *J. Quant. Spectrosc. Radiat. Transfer* **48,** 743 (1992).
9. B. D. Fried and S. D. Conte, ''The Plasma Dispersion Function,'' Academic Press, New York, 1961. (These authors consider the function $Z = i\sqrt{\pi}\ w$).
10. M. Abramowitz and I. A. Stegun, ''Handbook of Mathematical Functions,'' National Bureau of Standards, AMS55, New York, 1964.
11. A. K. Hui, B. H. Armstrong, and A. A. Wray, *J. Quant. Spectrosc. Radiat. Transfer* **19,** 509 (1978).
12. E. E. Whiting, *J. Quant. Spectrosc. Radiat. Transfer* **8,** 1379 (1968).
13. J. J. Olivero and R. L. Longbothum, *J. Quant. Spectrosc. Radiat. Transfer* **17,** 233 (1977).